

# Production of levulinic acid and ethyl levulinate from cellulosic pulp derived from the cooking of lignocellulosic biomass with active oxygen and solid alkali

Chen Gong\*, Junnan Wei\*, Xing Tang<sup>\*,\*\*,\*†</sup>, Xianhai Zeng<sup>\*,\*\*</sup>, Yong Sun<sup>\*,\*\*</sup>, and Lu Lin<sup>\*,\*\*,\*†</sup>

\*Xiamen Key Laboratory of Clean and High-valued Applications of Biomass, College of Energy, Xiamen University, Xiamen 361102, China

\*\*Fujian Engineering and Research Center of Clean and High-valued Technologies for Biomass, Xiamen 361005, Fujian, China

(Received 3 November 2018 • accepted 11 March 2019)

**Abstract**—Biomass-derived levulinic acid (LA) and its esters are currently envisaged as versatile, renewable platform chemicals. In this study, cellulosic pulp derived from the cooking of lignocellulosic biomass with active oxygen and solid alkali was employed as raw material for the formation of LA or ethyl levulinate (EL). This pretreatment process is highly effective for the delignification and deconstruction of lignocellulose matrix, making a facile degradation of the resulting cellulosic pulp to LA or EL. At this point, the acid-catalyzed hydrolysis or ethanolysis of cellulosic pulp was optimized by response surface methodology (RSM), offering desirable LA yield of 65.3% or EL yield of 62.7%, which is significantly higher than those obtained from raw biomass. More importantly, coking behavior on the inwall of the reactor was eliminated during the hydrolysis or ethanolysis of cellulosic pulp, which is one of the top challenges for the acid-catalyzed conversion of biomass in an industrial scale.

Keywords: Biomass, Pretreatment, Levulinic Acid, Ethyl Levulinate

## INTRODUCTION

Biomass resources are the only renewable carbon sources that can be used as the raw materials for the production of carbon-based chemicals and energy [1]. Lignocellulosic biomass, the most abundant biomass source, is mainly composed of cellulose (38-50%), hemicellulose (23-32%) and lignin (15-30%) [2]. Given the totally different chemical structure of these three components, the fractionation of lignocellulosic biomass is the prerequisite for the full use of these components. At this point, efficient and economical pretreatment process for the fractionation of lignocellulose is one of the top challenges for the development of a biorefinery.

At present, various physical, biological and/or chemical methods for the fractionation of lignocellulosic biomass components have been developed. The physical methods, such as the steam explosion method and the ammonia blasting method, are deemed as environmentally friendly, but these methods suffer from low efficiency and high cost [3,4]. Various microorganisms are used to degrade lignin from the lignocellulose matrix in mild conditions; however, microorganisms are highly sensitive to the external environment, and the above process is time-consuming [5,6]. Many chemical methods have also been proposed for the pretreatment of lignocellulosic biomass in various solvents. For example, ionic liquids and deep eutectic solvents [7-9] were recently employed as novel solvents for the fractionation of lignocellulose. However, the high cost of these solvents should be considered. Water is a green

and inexpensive solvent for delignification in the presence of sulfite or sodium hydroxide, which is widely used in traditional paper-making industry [10,11]. Nevertheless, toxic H<sub>2</sub>S or excessive alkali liquor forms during the above processes [12]. Recently, Lin et al. reported the fractionation of lignocellulosic biomass through cooking with active oxygen and solid alkali (CAOSA) in aqueous solution [13]. The microstructure of the lignocellulosic feedstock was thoroughly destroyed during the CAOSA process, and almost all the initial lignin was removed [14,15]. More importantly, the used alkali solid, such as MgO, can be easily recovered and reused in next run; therefore, CAOSA process is an efficient and clean strategy for the fractionation of lignocellulosic biomass.

The fractionation of lignocellulose is just the first step for a biorefinery; it is necessary to evaluate the downstream conversion of the resulting cellulosic pulp obtained from the CAOSA process. To this end, the conversion of the resulting cellulosic pulp into LA and its esters by acid-catalyzed hydrolysis and alcoholysis was investigated in this study. LA and its esters are currently considered as versatile biomass-derived platform chemicals that have a wide range of applications in fuel additives, fragrances, solvents, and polymers, etc. [16], and recent research has been done focusing on the production of LA and its esters from the vast range of carbohydrate-rich biomass, including lignocellulose biomass and microalgae [17-21]. Excitingly, desirable LA yield of 65.3% or ethyl levulinate (EL) yield of 62.7% was achieved by the acid-catalyzed hydrolysis or ethanolysis of cellulosic pulp through the optimization based on response surface methodology (RSM), which is significantly higher than that obtained from raw biomass. More importantly, coking behavior on the inwall of the reactor was eliminated during the hydrolysis or ethanolysis of cellulosic pulp, which is one of the top

<sup>†</sup>To whom correspondence should be addressed.

E-mail: x.tang@xmu.edu.cn, lulin@xmu.edu.cn

Copyright by The Korean Institute of Chemical Engineers.

challenges for the acid-catalyzed conversion of biomass in an industrial scale. These findings clearly indicate that the CAOSA process is not only an effective pretreatment for the fractionation of ligno-cellulose, but also is able to greatly facilitate the downstream conversion of the resulting cellulosic pulp.

## MATERIALS AND METHODS

### 1. Materials

Biomass raw materials used in this study include corncob, corn stalk, bamboo and corn straw, which were collected from Fujian Province, China; all these samples were air-dried, milled to obtain particles with a size lower than 1 mm for CAOSA process. Sulfuric acid (98%), formic acid (98%), acetic acid, ethanol magnesium oxide and calcium carbonate were purchased from Sinopharm Chemical Reagent Co. Ltd. (Shanghai, China). D-(+)-Glucose and D-xylose (98%) were purchased from Aladdin Reagent Co. Ltd. (Shanghai, China). Levulinic acid (99%), ethyl levulinate (99%) and furfural (98%) were supplied by Shanghai TCL.

### 2. Preparation of Cellulosic Pulp by CAOSA Process

Cellulosic pulp was prepared from various biomass raw materials by CAOSA process in a ball-shaped reactor with volume of 22 L (Fig. 1, Figs. S1 and S2). Taking bamboo for example, 1 kg bamboo sawdust, 5 kg water and 150 g MgO powder were charged into the ball-shaped reactor which was sealed and filled with O<sub>2</sub> (1.0 MPa). The reactor was heated to 170 °C at a ramp of 2 °C/min, and the CAOSA process was performed for 3 h at 170 °C. Thereafter, the resulting cellulosic pulp was separated from the reaction mixture by filtration, which was further washed with water and dried at 105 °C overnight. The production of cellulosic pulp from other



Fig. 1. Ball-shaped reactor for the production of cellulosic pulp by CAOSA process.

biomass raw materials by CAOSA process was conducted under the same reaction conditions. The composition of the biomass raw materials and the corresponding cellulosic pulp was analyzed by a two-step acid hydrolysis method based on TAPPI T249 cm-00 (2000) for cellulose and hemicellulose [22]. To be specific, 0.3 g sample and 3.0 mL 72% sulfuric acid (SA) was added into a test tube, which was then placed in water bath at 30 °C for 30 min. The resulting hydrolysate was diluted with 84 mL deionized water and then transferred into an autoclave, which was heated to 121 °C for 2 h. After cooling to room temperature, the resulting reaction mixture was neutralized with CaCO<sub>3</sub> and detected by high performance liquid chromatography to quantify the concentrations of glucose and xylose, and cellulose and hemicellulose content was calculated as follows. For the ash test, 10 g biomass was calcinated at 500 °C for 5 h; the residue was weighed, and the proportion of lignin was the rest part.

$$C_{\text{cellu}} = \frac{C_{\text{glu}} \div 0.998 \times 86.73 \times 0.90}{1000 \times m} \quad (1)$$

$$C_{\text{hemi}} = \frac{C_{\text{xyt}} \div 0.870 \times 86.73 \times 0.88}{1000 \times m} \quad (2)$$

where  $C_{\text{cellu}}$  is cellulose content (%),  $C_{\text{hemi}}$  is hemicellulose content (%),  $C_{\text{glu}}$  is glucose concentration (g/L),  $C_{\text{xyt}}$  is xylose concentration (g/L),  $m$  is the mass of biomass material (g).

### 3. Production of LA and EL from Raw Biomass Materials or Cellulosic Pulp

The hydrolysis and alcoholysis of raw biomass materials and cellulosic pulp were carried out in a 400 mL Hastelloy-C high-pressure reactor (Dalian-controlled Plant, Dalian, China). The reactor was heated in an adjustable electric stove, and the temperature of the reactor was monitored by a thermocouple connected to the reactor. To study LA yield from various materials, a reactor temperature of 200 °C was set and substrate (four kinds of biomass natural materials or pulps, 20 g), solvent (water, 300 g, liquid solid ratio 15 : 1 g/g), and catalyst (SA, 2 wt%, relative to solvent) were charged into the reactor and heated to the prescribed temperature for the desired reaction time of 30 min with stirring at 300 rpm. Taking bamboo and bamboo pulp as materials for single factor experiments, respectively, the major experimental conditions were set as follows: solvent water 300 mL, temperature (180-260 °C), SA concentration (1-5 wt%), liquid solid ratio (5 : 1-25 : 1 g/g), reaction time (10-50 min) [23,24]. On the other hand, production of EL in ethanol by bamboo pulp with extremely low SA as the catalyst was considered and the experimental conditions were set as follows: solvent ethanol 300 mL, temperature (180-220 °C), extremely low SA concentration (2-10 mmol/L), material concentration (20-60 g/L), and reaction time (90-210 min) [25-27]. After the end of experiments, the reactor to room temperature was immediately cooled by cool water bath and liquor and solid phase collected to be analyzed.

### 4. Optimization Based on RSM

The optimized trials of the preparation of LA and EL based on RSM were devised using Design Expert 8.0.6.1. The statistical parameters were estimated by multiple regression, and model quality was assessed by the correlation coefficient ( $R^2$ ) and analysis of variance

**Table 1. Independent variable values of LA production and their corresponding levels**

Independent variable	Symbol	Levels		
		-1	0	1
Temperature (°C)	X <sub>1</sub>	200	220	240
SA concentration (wt%)	X <sub>2</sub>	2	3	4
Liquid solid ratio (g/g)	X <sub>3</sub>	10 : 1	15 : 1	20 : 1
Reaction time (min)	X <sub>4</sub>	10	30	50

**Table 2. Independent variable values of EL production and their corresponding levels**

Independent variable	Symbol	Levels		
		-1	0	1
Temperature (°C)	X <sub>5</sub>	200	210	220
Material concentration (g/L)	X <sub>6</sub>	20	30	40
Reaction time (min)	X <sub>7</sub>	90	120	150

(ANOVA). The optimization process of LA yield mainly investigated the effects of these four factors: X<sub>1</sub> (temperature/T<sub>1</sub>, °C), X<sub>2</sub> (SA concentration/C, wt%), X<sub>3</sub> (liquid solid ratio/L, g/g), X<sub>4</sub> (reaction time/t<sub>1</sub>, min), and the optimization process of EL yield mainly investigated the effects of these three factors: X<sub>5</sub> (temperature/T<sub>2</sub>, °C), X<sub>6</sub> (material concentration/M, g/L), X<sub>7</sub> (reaction time/t<sub>2</sub>, min) [23,27]. For statistical calculation, the variables were coded according to Eq. (3):

$$X_{ik} = (X_i - X_0) / \Delta X \quad (3)$$

where X<sub>ik</sub> is the independent variable, X<sub>i</sub> is the real parameter value, X<sub>0</sub> is the real value of the midpoint, and ΔX is the gradient step value of the real parameter. Seven reaction factors could be calculated by Eqs. (4)-(10), and the reaction conditions of the RSM experiments were shown in Tables 1 and 2.

$$X_1 = (T_1 - 220) / 20 \quad (4)$$

$$X_2 = (C - 3) / 1 \quad (5)$$

$$X_3 = (L - 15) / 5 \quad (6)$$

$$X_4 = (t_1 - 30) / 10 \quad (7)$$

$$X_5 = (T_2 - 200) / 10 \quad (8)$$

$$X_6 = (M - 30) / 10 \quad (9)$$

$$X_7 = (t_2 - 150) / 30 \quad (10)$$

According to these results of RSM experiments, we could calculate the theoretical predicted LA yield based on Eq. (11).

$$Y = a_0 + \sum_{i=1}^4 a_i X_{ij} + \sum_{i=1}^4 \sum_{j=1}^4 a_{ij} X_i X_j \quad (11)$$

The regression coefficient could be calculated with the actual experimental results; the degree of influence of each factor could be found by the P-value of ANOVA. The simulation polynomial equation was to visualize the relationship between the corresponding levels of each factor and response data, then we could deter-

mine the optimum conditions [20].

## 5. Product Analysis

LA and other products in the filtrate obtained from the reaction were analyzed by high performance liquid chromatography (HPLC, WATERS Alliance e2695) with a Bio-Rad Aminex HPX-87H column (300×7.8 mm) and differential refraction detector 2414 manufactured by Waters Corp. of the United States. The column temperature was set at 60 °C, 5 mmol/L aqueous SA solution was used as the mobile phase with a flow rate of 0.6 mL/min, and the detection time was 60 min; the amount of inhalation per test was 10 μL. The external standard method was used to quantify the components and the standard materials used to quantify the product in hydrolysate, including LA (supplied by Shanghai TCI), formic acid (FA, supplied by Sinopharm Chemical Reagent Co. Ltd.), acetic acid (HAc, supplied by Sinopharm Chemical Reagent Co. Ltd.) and furfural (FF, supplied by Shanghai TCI). All standard materials used in HPLC were analytical reagent [28].

The amount of EL was determined on a gas chromatograph (GC, Agilent 6890 instrument) equipped with an HP-5 capillary column with dimensions of 30.0 m×320 μm×0.25 μm and a flame ionization detector operating at 270 °C. The external standard method was used to quantify the components and the standard material used to quantify the product in alcoholysate was EL (analytical reagent, supplied by Shanghai TCI) [29].

Biomass materials and hydrolysis residue were fixed to a metal-base specimen holder using double-sided sticky tape, and then coated with gold using a vacuum sputter-coater. Afterwards, scanning electron microscope (SEM) analysis of the studied samples (within 0.1 g) was performed on a SUPRA 55 SAPPHERE field emission scanning electron microscope at an accelerating voltage of 20 kV.

According to the test results, product yield was calculated by the following formulas:

$$\begin{aligned} \text{Yield based on weight of material (\%)} \\ = \frac{\text{product content (g)}}{\text{material content (g)}} \times 100\% \end{aligned} \quad (12)$$

$$\begin{aligned} \text{Yield based on theoretical yield (\%)} \\ = \frac{\text{desired product in reaction product (g)}}{\text{desired product in raw material (g)}} \times 100\% \end{aligned} \quad (13)$$

## RESULTS AND DISCUSSION

### 1. Composition and Structure of the Raw Materials and their Cellulosic Pulps

The main component changes of the studied natural materials and the corresponding CAOSA pulps were measured, and the quantified results listed in Table 3. Obviously, after the pretreatment of CAOSA process, the proportion of lignin in natural materials was significantly decreased and the proportion of cellulose was remarkably increased, which indicated that the CAOSA process had a good effect on delignification of lignin with different biomass materials. For instance, about 27.5% of cellulose proportion increase of corn cob was detected, and almost all of lignin (88.5%) lost after the CAOSA process; the loss of lignin component of other natural materials exhibited similar tendency to that of corn cob. In

**Table 3. Composition of biomass materials and their cellulosic pulps**

Entry	Materials	Cellulose (%) <sup>a</sup>	Hemicellulose (%)	Lignin (%)	Ash (%)	Pulp yield (%)
1	Corn cob	33.2	26.8	32.7	7.3	/
2	Corn cob pulp	60.7	23.5	8.4 (88.5 <sup>b</sup> )	7.4	44.9
3	Corn straw	35.7	25.8	30.0	8.5	/
4	Corn straw pulp	64.3	23.4	5.2 (92.6 <sup>b</sup> )	7.1	42.7
5	Bamboo	44.8	23.7	26.9	4.6	/
6	Bamboo pulp	72.7	20.3	3.7 (93.2 <sup>b</sup> )	3.3	49.7
7	Wheat straw	41.5	25.6	26.5	6.4	/
8	Wheat straw pulp	66.5	23.1	6.2 (89.0 <sup>b</sup> )	4.2	47.1

Cooking reaction condition: 1 kg biomass, 150 g MgO, liquid solid ratio 5 : 1 g/g, 1.0 MPa O<sub>2</sub>, 170 °C, 70 min

<sup>a</sup>Contents based on the oven-dried weight of biomasses or their pulps

<sup>b</sup>The data in parentheses are the delignification rate after the cooking process

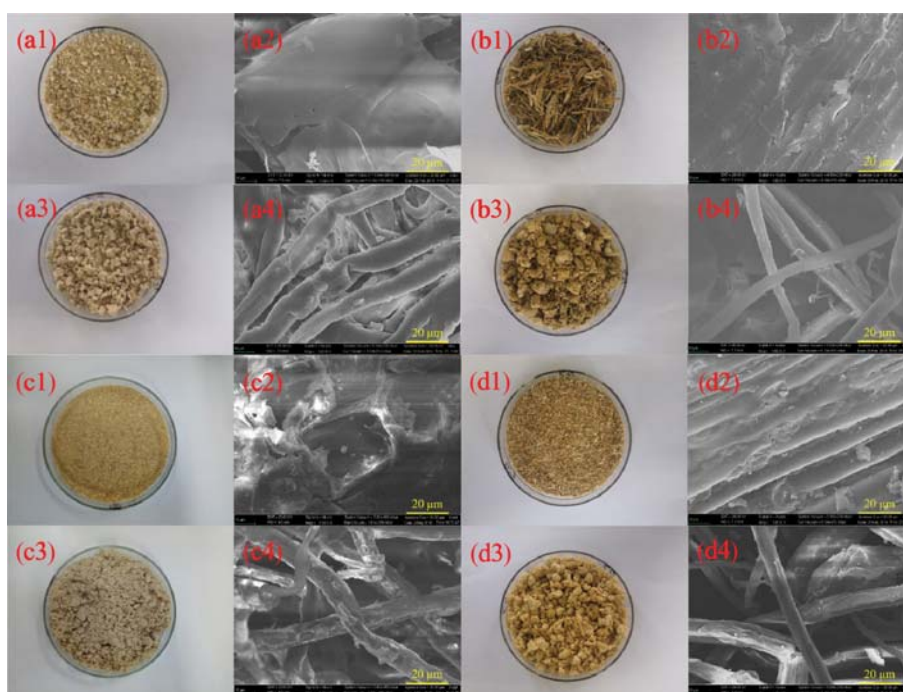


**Fig. 2. The photos and SEM images of biomass materials and their cellulosic pulps. (a1)-(a4): Corn cob and corn cob pulp. (b1)-(b4): Corn straw and corn straw pulp. (c1)-(c4): Bamboo and bamboo pulp. (d1)-(d4): Wheat straw and wheat straw pulp.**

addition, the pulp yields of these four kinds of biomass material were all range in 40-50%, and this demonstrated that most of cellulose was reserved after CAOSA process.

To investigate the structural change of raw biomass after cooking, the morphologies of representative biomass materials and their pulps were analyzed by SEM. As shown in Fig. 2, an obvious large fiber or cell wall structure of raw materials could be clearly observed (Figs. 2(a2), (b2), (c2) and (d2)). In comparison, the original cell wall structure was completely destroyed and the tiny fibers were exposed and randomly stacked together in the biomass pulp obtained by CAOSA process (Figs. 2(a4), (b4), (c4) and (d4)). The loose structure of fibers in the biomass pulp could facilitate the interaction between the catalyst and fibers, which further promoted the acid-catalyzed hydrolysis of cellulose to form LA. Consequently, biomass pulps could be employed as a desirable starting

material for the production of LA, which will be discussed in detail later.

## 2. Production of LA from Various Raw Biomass Materials and their Cellulosic Pulps

These above biomass feedstocks and their corresponding pulps were used as substrates to produce LA under 200 °C for 30 min, and the typical liquid chromatogram of major products in biomass hydrolysate was demonstrated in Fig. S3. As shown in Table 4, an LA yield of 10.0% was achieved from corn cob at 200 °C for 30 min, which obviously indicated that side reactions occurred during the degradation of corn cob. The main detected by-products in liquid products involved FA, HAc and FF. When corn cob pulp was used as the substrate, the yields of LA and FA were improved to 22.5% and 10.0%, respectively, while little HAc and FF were detected in liquid products. Similarly, LA and FA yields of other

**Table 4.** The products derived from hydrolysis of biomass materials and their cellulosic pulps

Entry	Substrate	LA (%)	FA (%)	HAc (%)	FF (%)	Residues (%)
1	Corn cob	10.0	4.5	5.5	8.5	31.5
2	Corn cob pulp	22.5	10.0	0	1.0	16.0
3	Corn straw	11.5	5.0	5.0	6.5	28.5
4	Corn straw pulp	24.5	11.5	0	0.5	11.5
5	Bamboo	14.0	5.5	4.5	5.5	22.5
6	Bamboo pulp	28.5	12.0	0	1.0	11.0
7	Wheat straw	12.0	5.5	5.5	7.0	25.5
8	Wheat straw pulp	20.0	11.5	0	1.5	17.5

Reaction conditions: 300 g water, 200 °C, SA concentration 2 wt%, liquid solid ratio 15 : 1 g/g, 30 min

Yield based on weight of substrate material

biomass pulps (corn straw pulp, bamboo pulp and wheat straw pulp) were much higher than those of their natural materials under the studied conditions, and the detected HAc and FF obtained from pulps were negligible. In general, HAc and furfural FF were generated from hemicellulose. Specifically, HAc was produced through the hydrolysis of acetyl groups linked to sugars, and FF was formed via the decomposition of xylose [30]. Because the CAOSA process was performed in the presence of O<sub>2</sub> at 160 °C, acetyl groups in hemicellulose could be easily converted to HAc and hydroxyacetic acid (Fig. S4). Therefore, no HAc was formed during the acid-catalyzed hydrolysis of the resulting cellulosic pulps. On the other hand, the removal of lignin by CAOSA process resulted in

fluffy fiber structure in the cellulosic pulps (Fig. 2), which could allow the rapid conversion of hemicellulose FF in the presence of acid catalyst. However, the resulting FF could readily convert to by-products like humins in the presence of acid catalysts, and then gave a relatively low FF yield from cellulosic pulp compared to the raw biomass (Table 4). To verify this assumption, the acid-catalyzed hydrolysis of bamboo pulp was immediately stopped once the temperature reached 200 °C (reaction time 0 min); the liquid chromatogram of products is provided in Fig. S5. At this point, FF yield of 4.5% was measured, which was higher than that obtained after prolonging the reaction time to 30 min (Table 4, entry 6). The above phenomenon could be attributed to the more cellulose content in

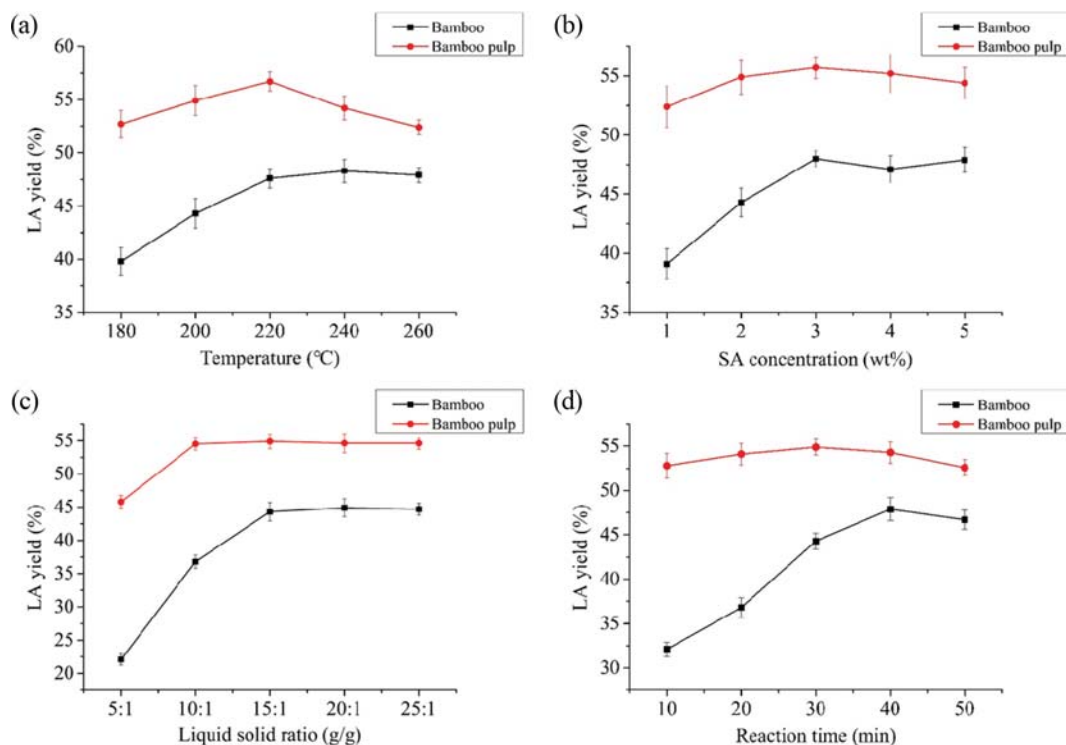


**Fig. 3.** Effect of factors in LA production from bamboo and bamboo pulp. (a): Reaction conditions: 300 g water, SA concentration 2 wt%, liquid solid ratio 15 : 1 g/g, 30 min. (b): Reaction conditions: 300 g water, 200 °C, liquid solid ratio 15 : 1 g/g, 30 min. (c): Reaction conditions: 300 g water, 200 °C, SA concentration 2 wt%, 30 min. (d): Reaction conditions: 300 g water, 200 °C, SA concentration 2 wt%, liquid solid ratio 15 : 1 g/g. LA yield based on theoretical yield.

biomass pulps and its facile hydrolysis resulting from the effective delignification. In addition, residues generated from biomass pulp were less than those of raw biomass.

### 3. Single Factor Comparison of LA and EL Production from Bamboo or Bamboo Pulp

Fig. 3 illustrates the effect of temperature, SA concentration, material concentration and time on the production of LA from bamboo or bamboo pulp. It was found that bamboo pulp offered a high LA yield than that given by bamboo under the same conditions. An LA yield of 52.7% was obtained from bamboo pulp at 180 °C, approximately 13% higher than that derived from natural bamboo (Fig. 3(a)). With the increase of temperature up to 220 °C, LA yield for bamboo and its pulp was improved to 47.6% and 56.7%, respectively. Nevertheless, if the temperature was further increased, LA yield of bamboo almost remained unchanged and the LA yield of its pulp even sharply decreased, probably owing to the transformation and degradation of LA at a temperature higher than 220 °C. LA yield of bamboo sharply increased from 39.1% to 48.0% with the increasing concentration of SA from 1 wt% to 3 wt%, but the yield of LA cannot be further improved even if adding more SA into the reaction mixtures (Fig. 3(b)). Interestingly, the desired LA yield of 52.4% was obtained from bamboo pulp at a SA concentration of just 1 wt%, and the LA yield of pulp could be improved to 55.7% with the increase of SA concentration to 3 wt%. The excessive SA (>3 wt%) could impair the LA yield of bamboo pulp, and probably cause serious corrosion to the metal reactor. Material concentration was also a non-negligible parameter that had an

impact on the conversion of bamboo or bamboo pulp to LA (Fig. 3(c)). LA yield of bamboo increased with material concentration and then reached a plateau and was maintained at 44.7%. The effect of liquid solid ratio on LA yield of bamboo pulp exhibited a similar trend to that of natural bamboo, but a high LA yield was achieved from bamboo pulp at the condition of same liquid solid ratio. The influence of reaction time on the LA yield of bamboo showed a similar trend to that of temperature (Fig. 3(d)). For example, bamboo was converted to LA at a yield of 32.1% at 200 °C in 10 min, and the LA yield increased to 47.9% with prolonged reaction time from 10 to 40 min. The formation of LA was accelerated if bamboo was transformed into pulp as substrate; consequently, the LA yield reached 52.8% at the same temperature within 10 min. However, LA yield of bamboo pulp remained nearly unchanged with the prolongation of reaction time, and it was obvious that bamboo pulp needed less time to be hydrolyzed completely relative to natural bamboo. Therefore, compared to raw biologic materials, biomass pulp seemed to be a superior substrate for the formation of LA under the mild conditions.

We also studied the effect of temperature, SA concentration, initial material concentration and reaction time on the EL production from bamboo pulp (Fig. 4). In Fig. 4(a), EL yield increased with the temperature in the range of 180–200 °C; however, a higher temperature facilitated the transformation of EL or the formation of by-products. SA concentration was one of the most key parameters for the EL production from bamboo pulp (Fig. 4(b)). The yield of EL remarkably increased from 4.8% to 62.2% when the SA con-

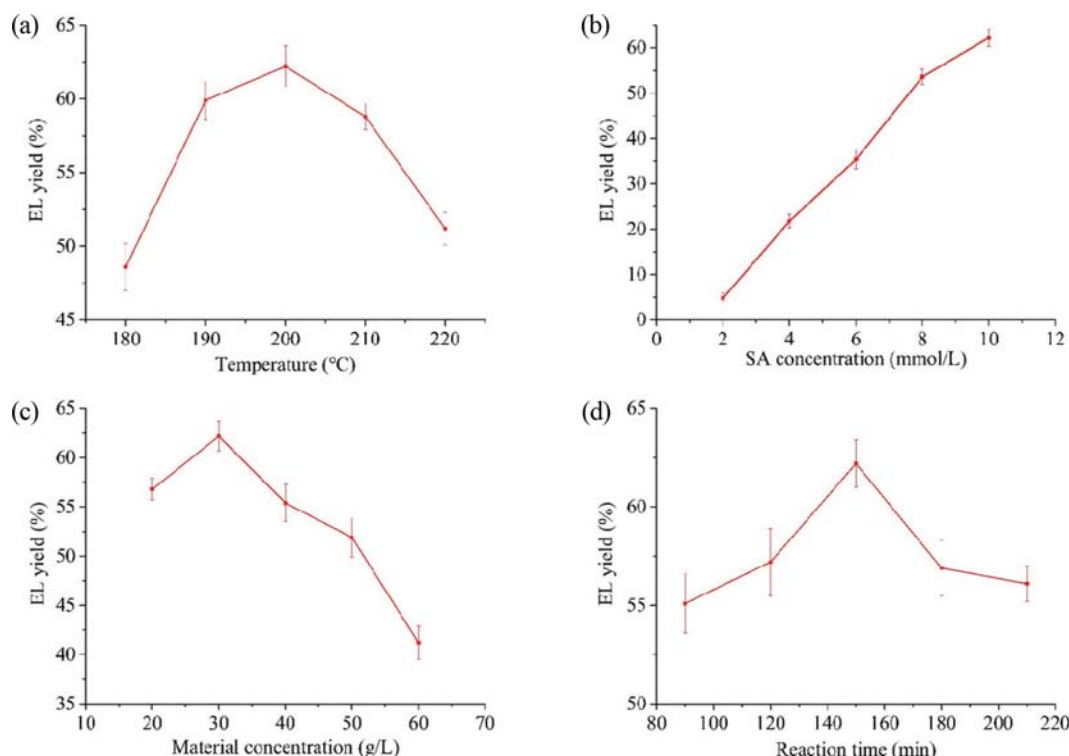


Fig. 4. Effect of factors in EL production from bamboo pulp. (a): Reaction conditions: 300 mL ethanol, SA concentration 10 mmol/L, material concentration 30 g/L, 150 min. (b): Reaction conditions: 300 mL ethanol, 210 °C, material concentration 30 g/L, 150 min. (c): Reaction conditions: 300 mL ethanol, 210 °C, SA concentration 10 mmol/L, 150 min. (d): Reaction conditions: 300 mL ethanol, 210 °C, SA concentration 10 mmol/L, material concentration 30 g/L. EL yield based on theoretical yield.

centration was increased from 2 mmol/L to 10 mmol/L, Therefore, under the circumstance of extremely low SA ( $\leq 10$  mmol/L) condition, SA concentration of 10 mmol/L was the best choice to produce EL by bamboo pulp [25,26]. As the concentration of bamboo pulp increased from 20 g/L to 30 g/L, the EL yield was improved from 56.8% to 62.2% at 210 °C in 150 min; with the further increase in the pulp loading amount, a gradual decrease in EL yield was observed, indicating the biomass pulp not being adequately alcoholized (Fig. 4(c)). The reaction results as functions of the reaction time are depicted in Fig. 4(d). Similar to the effect of temperature, as the reaction time increased in the range of 90-210 min, the EL yield showed a volcano-like trend with a maximal value of 62.2% achieved at 210 °C in 150 min.

#### 4. RSM Experiments and Analysis

Based on the results of single factor experiments, we could get the reference values of the response surface analysis and the level of the reference values (Tables 1 and 2). Each parameter and its horizontal value were entered into the Box-Behnken model of the response surface system (three or four parameters, three levels). For LA production, a total of 27 sets of test schemes were generated, with 24 groups as the analyzed test and 3 groups as the cen-

**Table 5. Design and results of the RSM of LA production**

Trial	X <sub>1</sub>	X <sub>2</sub>	X <sub>3</sub>	X <sub>4</sub>	LA yield (%)
1	0	0	0	0	64.1
2	-1	0	1	0	53.5
3	0	0	1	-1	55.7
4	0	-1	-1	0	29.1
5	0	1	1	0	59.1
6	1	-1	0	0	53.2
7	0	0	-1	1	42.1
8	0	1	0	-1	60.9
9	1	0	1	0	58.8
10	0	-1	0	-1	55.5
11	0	-1	1	0	47.2
12	0	0	0	0	63.7
13	0	1	-1	0	54.6
14	-1	-1	0	0	55.1
15	0	0	1	1	46.1
16	1	1	0	0	58.8
17	-1	0	-1	0	53.1
18	-1	0	0	-1	59.2
19	0	-1	0	1	56.6
20	0	0	-1	-1	33.8
21	1	0	0	1	56.3
22	1	0	0	-1	57.3
23	0	1	0	1	55.8
24	1	0	-1	0	52.8
25	-1	1	0	0	55.4
26	0	0	0	0	63.5
27	-1	0	0	1	59.8

X<sub>1</sub>: Temperature (°C), X<sub>2</sub>: SA concentration (wt%), X<sub>3</sub>: Liquid solid ratio (g/g), X<sub>4</sub>: Reaction time(min)  
LA yield based on theoretical yield

tral test. For EL production, a total of 17 sets of test schemes were generated, with 12 groups as the analyzed test and 5 groups as the central test [31]. The results are shown in Tables 5 and 6.

**Table 6. Design and results of the RSM of EL production**

Trial	X <sub>5</sub>	X <sub>6</sub>	X <sub>7</sub>	EL yield (%)
1	0	0	0	62.2
2	1	1	0	50.2
3	0	0	0	62.1
4	0	0	0	62.3
5	-1	-1	0	57.5
6	0	-1	1	56.9
7	-1	0	-1	51.2
8	0	-1	-1	55.1
9	1	0	1	55.5
10	0	0	0	61.9
11	0	1	-1	50.9
12	1	0	-1	52.7
13	0	1	1	55.1
14	0	0	0	62.0
15	1	-1	0	59.9
16	-1	1	0	49.8
17	-1	0	1	57.8

X<sub>5</sub>: Temperature (°C), X<sub>6</sub>: Material concentration (g/L), X<sub>7</sub>: Reaction time (min)  
EL yield based on theoretical yield

**Table 7. ANOVA results of the RSM of LA production**

Source	Sum of square	Degree of freedom	Mean square	F-value	P-value
Model	1517.35	14	108.38	3.35	0.0212
X <sub>1</sub>	3.20	1	3.20	0.099	0.7585
X <sub>2</sub>	265.08	1	265.08	8.19	0.0143
X <sub>3</sub>	251.17	1	251.17	7.76	0.0165
X <sub>4</sub>	2.71	1	2.71	0.084	0.7774
X <sub>1</sub> X <sub>2</sub>	2.56	1	2.56	0.079	0.7833
X <sub>1</sub> X <sub>3</sub>	7.84	1	7.84	0.24	0.6315
X <sub>1</sub> X <sub>4</sub>	0.64	1	0.64	0.020	0.8905
X <sub>2</sub> X <sub>3</sub>	46.24	1	46.24	1.43	0.2551
X <sub>2</sub> X <sub>4</sub>	9.61	1	9.61	0.30	0.5958
X <sub>3</sub> X <sub>4</sub>	80.10	1	80.10	2.47	0.1417
X <sub>1</sub> <sup>2</sup>	15.79	1	15.79	0.49	0.4982
X <sub>2</sub> <sup>2</sup>	174.55	1	174.55	5.39	0.0386
X <sub>3</sub> <sup>2</sup>	769.07	1	769.07	23.76	0.0004
X <sub>4</sub> <sup>2</sup>	153.13	1	153.13	4.73	0.0503
Residual	388.46	12	32.37	-	-
Lack of fit	387.74	10	38.77	107.70	0.0092
Pure error	0.72	2	0.36	-	-
Total	1905.81	26	-	-	-

X<sub>1</sub>: Temperature (°C), X<sub>2</sub>: SA concentration (wt%), X<sub>3</sub>: Liquid solid ratio (g/g), X<sub>4</sub>: Reaction time (min)  
P-value<0.05, significant; P-value<0.01, extremely significant

**Table 8. ANOVA results of the RSM of EL production**

Source	Sum of square	Degree of freedom	Mean square	F-value	P-value
Model	315.23	9	35.03	12.73	0.0015
X <sub>5</sub>	69.29	1	69.29	25.18	0.0015
X <sub>6</sub>	0.51	1	0.51	0.18	0.6810
X <sub>7</sub>	29.89	1	29.89	10.86	0.0132
X <sub>5</sub> X <sub>6</sub>	0.99	1	0.99	0.36	0.5682
X <sub>5</sub> X <sub>7</sub>	1.41	1	1.41	0.51	0.4978
X <sub>6</sub> X <sub>7</sub>	3.55	1	3.55	1.29	0.2936
X <sub>5</sub> <sup>2</sup>	59.48	1	59.48	21.61	0.0023
X <sub>6</sub> <sup>2</sup>	66.52	1	66.52	24.17	0.0017
X <sub>7</sub> <sup>2</sup>	61.55	1	61.55	22.36	0.0021
Residual	19.27	7	2.75	-	-
Lack of fit	19.13	3	6.38	193.52	<0.0001
Pure error	0.13	4	0.033	-	-
Total	334.50	16	-	-	-

X<sub>5</sub>: Temperature (°C), X<sub>6</sub>: Material concentration (g/L), X<sub>7</sub>: Reaction time (min)

P-value<0.05, significant; P-value<0.01, extremely significant

ANOVA results (Tables 7 and 8) were used to test the statistical significance of the quadratic equation model of the primary item, quadratic term, and interaction item (surface effect). A larger F-value and smaller P-value indicated a higher significance of the corresponding variable [32]. In addition, the multiple coefficients of correlation  $R^2 > 0.9$  indicated a close agreement between experimental and predict values of the LA and EL yields (Fig. 5).

In Table 7, the P-value of the Box-Behnken model was 0.0212, and the lack of fit P-value was 0.0092, indicating that the response surface regression model was valid. In the primary item, items X<sub>2</sub> and X<sub>3</sub> were statistically significant ( $P_{X_2}=0.0143$ ,  $P_{X_3}=0.0165$ ). In the quadratic term, item X<sub>3</sub><sup>2</sup> reached an extremely significant level ( $P=0.0004$ ); items X<sub>2</sub><sup>2</sup> and X<sub>4</sub><sup>2</sup> were also statistically significant ( $P_{X_2}=0.0386$ ,  $P_{X_4}=0.0503$ ). For the interaction item, X<sub>3</sub>X<sub>4</sub> was the most statistically significant among them ( $P=0.1417$ ). Other items were not statistically significant.

In Table 8, the P-value of the Box-Behnken model was 0.0015,

and the lack of fit P-value was less than 0.0001, which showed a better significance than that of Table 7. Items X<sub>5</sub> and X<sub>7</sub> were statistically significant in the primary item ( $P_{X_5}=0.0015$ ,  $P_{X_7}=0.0132$ ). In the quadratic term, all items were statistically significant ( $P_{X_5}^2=0.0023$ ,  $P_{X_6}^2=0.0017$ ,  $P_{X_7}^2=0.0021$ ), and for the interaction item, none of them was statistically significant.

By comparing the data in Tables 7 and 8, the quadratic multiple regressions of Eq. (11) were obtained as follows:

$$Y_{LA} = 65.10 + 0.52X_1 + 4.70X_2 + 4.58X_3 - 0.48X_4 - 0.80X_1X_2 + 1.40X_1X_3 - 0.40X_1X_4 - 3.40X_2X_3 - 1.55X_2X_4 - 4.48X_3X_4 - 1.72X_1^2 - 5.72X_2^2 - 12.01X_3^2 - 5.36 \quad (14)$$

$$Y_{EL} = 62.09 - 2.94X_5 + 0.25X_6 + 1.93X_7 - 0.50X_5X_6 + 0.59X_5X_7 - 0.94X_6X_7 - 3.76X_5^2 - 3.97X_6^2 - 3.82X_7^2 \quad (15)$$

3D response surface and contour map of the interaction of factors (Figs. 6, 7 and 8) were considered as fixed factors, with the center value being unchanged, and the interaction of the other two factors affecting LA and EL yield. Generally speaking, there were two possible geometrical shapes of a contour map; an elliptical contour indicated that the interactions of factors were significant, and a circle contour indicated that the interactions were not significant [20,33].

The interaction relationships of temperature (X<sub>1</sub>) with SA concentration (X<sub>2</sub>), liquid solid ratio (X<sub>3</sub>) and reaction time (X<sub>4</sub>) on LA yield are shown in Fig. 6(a), 6(b) and 6(c), respectively. These three contour maps were all elliptical and indicated that the interactions of temperature with the other three factors were statistically significant. When temperature was constant, LA yield decreased with a change in the other three factors from 0 to -1 or 1, mainly because low SA concentration was harmful to catalytic efficiency and high SA concentration led to more generation of by-product; too high or too low liquid solid ratio affected the uniformity of temperature resulting in LA yield decline, and reaction time controlled the holding time in a specific temperature. On the contrary, LA yield changed limited to temperature changed when other three factors were constant, indicating that temperature had a negligible effect on LA yield relative to other factors.

Fig. 7(a) and 7(b) show the interaction relationships of SA concentration (X<sub>2</sub>) with liquid solid ratio (X<sub>3</sub>) and reaction time (X<sub>4</sub>)

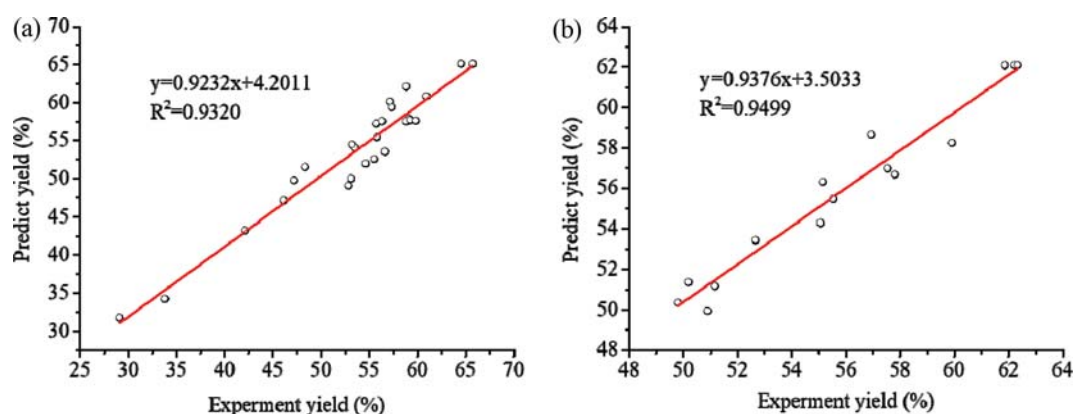


**Fig. 5. Relationship between predicted values and experimental values of LA (a) and EL (b) production.**

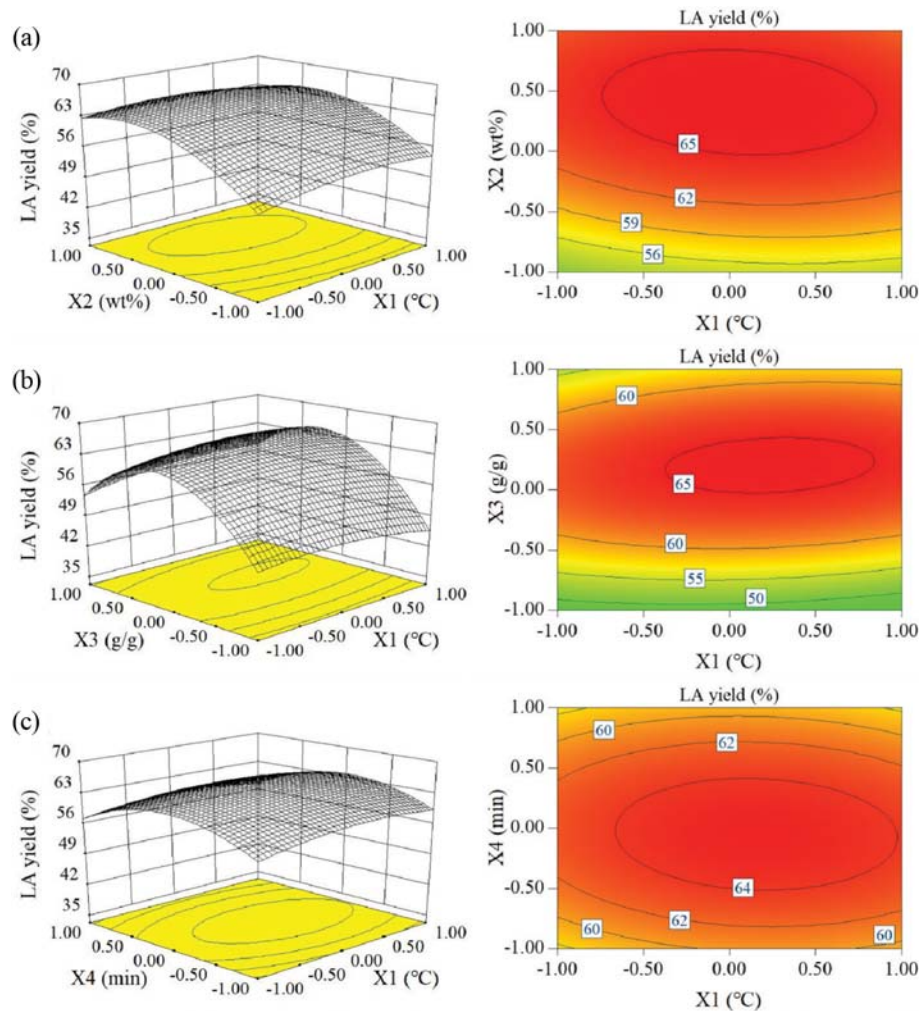


**Fig. 6. Reciprocal interaction of temperature with SA concentration, liquid solid ratio and reaction time on LA production.**  $X_1$ : Temperature ( $^{\circ}\text{C}$ ),  $X_2$ : SA concentration (wt%),  $X_3$ : Liquid solid ratio (g/g),  $X_4$ : Reaction time(min). (a): Reciprocal interaction of temperature with SA concentration. (b): Reciprocal interaction of temperature with liquid solid ratio. (c): Reciprocal interaction of temperature with reaction time.

on LA yield, respectively. The contour maps show that the interaction of SA concentration with liquid solid ratio was statistically significant, and the interaction of SA concentration with reaction time was not significant relatively. The 3D maps were completely convex surfaces and demonstrated that when SA concentration or other two factors was constant, an increase in the interaction point decreased LA yield. If SA concentration was too high or too low, the by-products in the reaction system might increase gradually or the reaction was incomplete, resulting in LA decomposition or low yield; therefore, selecting an appropriate SA concentration value was very important in LA production.

Fig. 7(c) is about the interaction relationships of liquid solid ratio ( $X_3$ ) with reaction time ( $X_4$ ) on LA yield, and the contour map demonstrates that the interaction of liquid solid ratio and reaction time was not very significant. Specifically, liquid solid ratio affected the mass transfer efficiency, and reaction time determined whether the reaction was complete, which means the degree of LA production was determined by adjusting the combination of these two factors.

As for EL production, the interaction relationships of temperature ( $X_5$ ), material concentration ( $X_6$ ) and reaction time ( $X_7$ ) on EL yield are shown in Fig. 8(a), 8(b) and 8(c), respectively. Demonstrated by 3D surface, every factor in EL production had a distinct quadratic effect on EL yield, which signified that EL yield was unstable and could be affected by the change of reaction condition easily, and these factors played a similar role in EL preparation as in LA production, theoretically. Therefore, the reaction condition should be accurately controlled in EL production to reach relatively higher EL yield.

The optimal point of reaction condition was further determined by the ridge max analysis. The method of ridge analysis computed the estimated ridge of maximum response for increasing radius from the center of original design [34]. The ridge max analysis indicated that maximum LA yield was 66.5%, and the corresponding optimum conditions were temperature  $223.2^{\circ}\text{C}$ , SA concentration 3.37 wt%, liquid solid ratio 15.9 : 1, reaction time 28.2 min; on the other hand, maximum yield of EL yield under the circumstance of extremely low SA (10 mmol/L) was 62.9%, and the corresponding

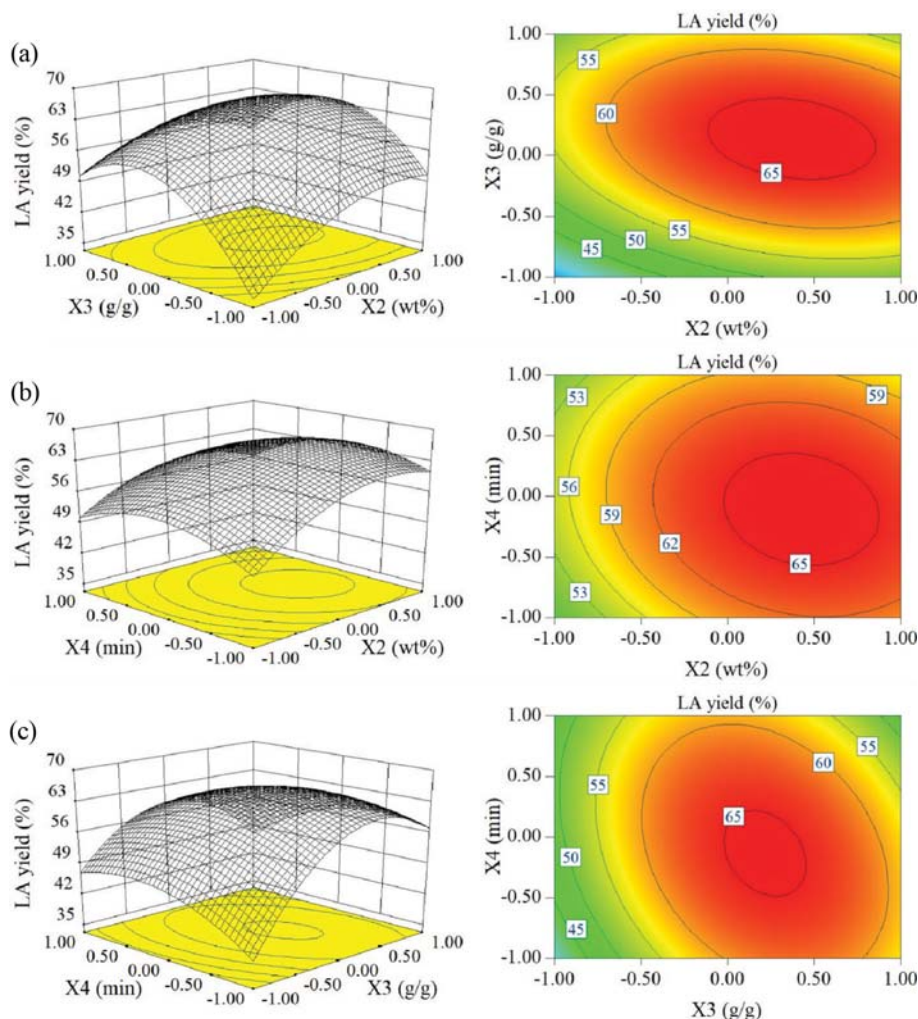


Fig. 7. Reciprocal interaction of SA concentration, liquid solid ratio and reaction time on LA production.  $X_2$ : SA concentration (wt%),  $X_3$ : Liquid solid ratio (g/g),  $X_4$ : Reaction time (min). (a): Reciprocal interaction of SA concentration with liquid solid ratio. (b): Reciprocal interaction of SA concentration with reaction time. (c): Reciprocal interaction of liquid solid ratio with reaction time.

optimum conditions were temperature 210.3 °C, material concentration 26.2 g/L, reaction time 126.6 min. To confirm the predicted results, two verification tests were performed under the optimum conditions, and LA yield 65.3% and EL yield 62.7% were obtained. In addition, LA yield 54.7% and EL yield 51.3% were obtained if we used bamboo as material in the same reaction conditions.

Some related results in the representative literature for the production of LA or EL from cellulose or biomass with pretreatment are shown in Table S1. It can be seen that the pretreatment of cellulose in ionic liquid was effective to improve the yield of LA. Unfortunately, the high cost limited the application of ionic liquid on a large scale. In this work, CAOSA was employed as a pretreatment method for lignocellulosic biomass due to its low cost and effectiveness for delignification, which could offer a relatively high LA yield from the resulting cellulosic pulp by acid-catalyzed hydrolysis. EL yield of 62.7% was also achieved from bamboo pulp obtained by the CAOSA process, which was higher than that obtained from other biomass materials without any pretreatment. These results suggest that CAOSA is an efficient method for the pretreatment of

lignocellulosic biomass to produce LA and EL.

### 5. Study on Coking Behavior

Coking behavior is common during the acid-catalyzed conversion of biomass, which is one of the top challenges on an industrial scale. To investigate the coking behavior of the degradation of bamboo and its pulp, photos and SEM images of their hydrolysis residue were supplied in Fig. 9. When natural bamboo was directly applied to produce LA under the experimental conditions, bamboo was heavily carbonized and the formed coke adhered to the agitator (Fig. 9(a) and 9(b)). Interestingly, much less carbon deposits formed if the pulp was used as the substrate for the production of LA (Fig. 9(d) and 9(e)), making the reactor easier to clean. The morphology of these two types of residues was further investigated by SEM images (Fig. 9(c) and 9(f)). Obviously, both bamboo hydrolysis residue and bamboo pulp hydrolysis residue were composed of spherical crystal particles, but the size of particles of bamboo pulp hydrolysis residue was smaller than that of bamboo hydrolysis residue, probably resulting in the facile removal of the bamboo pulp residue.

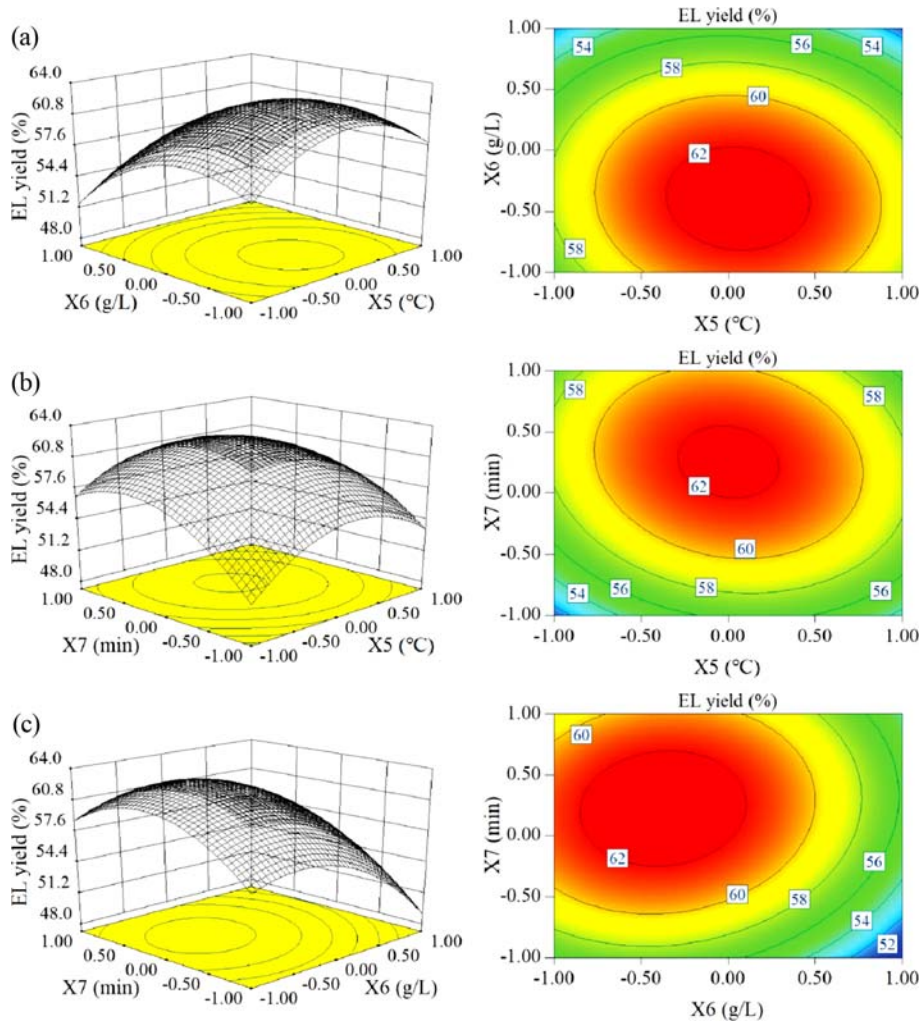


Fig. 8. Reciprocal interaction of temperature, material concentration and reaction time on EL production. X<sub>5</sub>: Temperature (°C), X<sub>6</sub>: Material concentration (g/L), X<sub>7</sub>: Reaction time (min). (a): Reciprocal interaction of temperature with material concentration. (b): Reciprocal interaction of temperature with reaction time. (c): Reciprocal interaction of material concentration with reaction time.

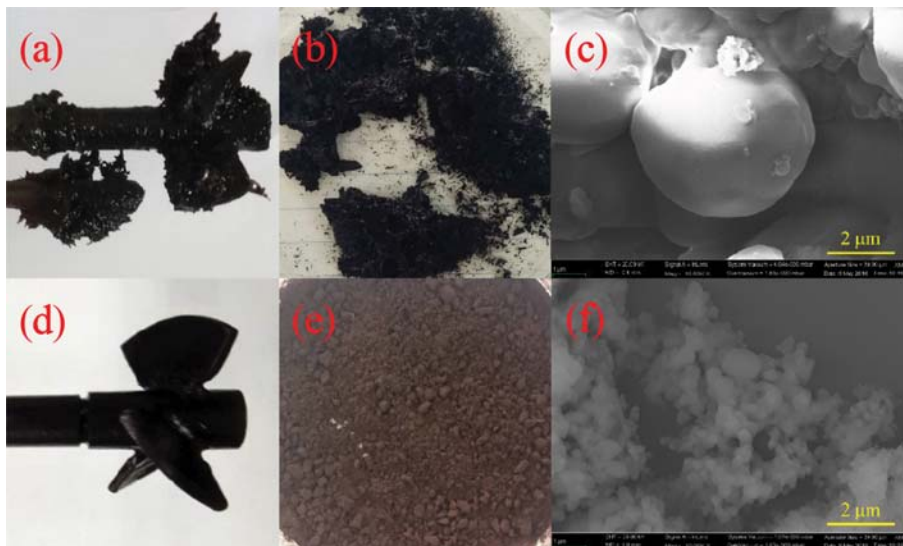


Fig. 9. The photos and SEM images of bamboo and bamboo pulp hydrolysis residue. (a)-(c): bamboo hydrolysis residue. (d)-(e): bamboo pulp hydrolysis residue. (f) is an SEM image of bamboo pulp residue.

## CONCLUSIONS

The lignin in biomass feedstocks, including corn cob, corn straw, bamboo and wheat straw, was effectively removed through CAOSA process, and then the corresponding biomass pulp with more cellulose components was obtained. Bamboo pulp is one of the representative biomass pulps that can be employed as the raw material for the production of LA and its esters. The constitutional unit of bamboo pulp was proved smaller than that of bamboo, indicating the pulp having higher surface area. Consequently, biomass pulp with greater amount of cellulose and higher surface area exhibited a better performance on the hydrolysis/alcoholysis to yield LA or EL. The reaction parameters for the formation of LA or EL from bamboo pulp were optimized by the RSM experiments, offering desirable LA yield of 65.3% or EL yield of 62.7%, which is remarkably higher than that obtained from raw biomass. In addition, the pretreatment of CAOSA enhances the anti-coking ability of the pulp during the acid-catalytic process, making the biomass pulp residues easier to wash off. Therefore, we believe this work will stimulate a wide interest of research on the formation of other valuable derivatives from the studied biomass pulps.

## ACKNOWLEDGEMENTS

We are grateful for funding by the National Natural Science Foundation of China (Grant Nos. 21676223; 21706223; 21776234), the Natural Science Foundation of Fujian Province of China (Grant Nos. 2018J01017), the PetroChina Innovation Foundation (No. 2018D-5007-0503) and the Energy Development Foundation of Energy College, Xiamen University (Grant No. 2017NYFZ02).

## NOMENCLATURE

### Alphabetic Letters

ANOVA	: analysis of variance
C	: SA concentration in LA production [wt%]
CAOSA	: cooking with active oxygen and solid alkali
$C_{cellu}$ and $C_{hemi}$	: content of cellulose and hemicellulose [%]
$C_{glu}$ and $C_{xy}$	: concentration of glucose and xylose [g/L]
EL	: ethyl levulinate
FA	: formic acid
FF	: furfural
GC	: gas chromatography
HAc	: acetic acid
HPLC	: high performance liquid chromatography
L	: liquid solid ratio [g/g]
LA	: levulinic acid
M	: material concentration in EL production [g/L]
m	: the mass of biomass [g]
$R^2$	: the correlation coefficient
RSM	: response surface methodology
SA	: sulfuric acid
SEM	: scanning electron microscope
$T_1$ and $T_2$	: temperature of LA and EL production [°C]
$t_1$ and $t_2$	: reaction time of LA and EL production [min]
X	: level of independent variable or real parameter value

$Y$ ,  $Y_{LA}$  and  $Y_{EL}$ : predicted response, predicted response of LA and EL yield

### Greek Letters

$\Delta X$ : the gradient step value of the real parameter

## SUPPORTING INFORMATION

Additional information as noted in the text. This information is available via the Internet at <http://www.springer.com/chemistry/journal/11814>.

## REFERENCES

- Z. Tan, K. Chen and P. Liu, *Renew. Sust. Energy Rev.*, **41**, 368 (2015).
- F. D. Pileidis and M. M. Titirici, *ChemSusChem*, **9**, 562 (2016).
- R. Kataria, A. Mol, E. Schulten, A. Happel and S. I. Mussatto, *Ind. Crops Prod.*, **106**, 48 (2017).
- W. Apiwatanapiwat, P. Vaithanomsat, S. Ushiwaka, K. Morimitsu, M. Machida, W. Thanapase, Y. Murata and A. Kosugi, *Biomass Convers. Bior.*, **6**, 181 (2016).
- G. Janusz, A. Pawlik, J. Sulej, U. Świdarska-Burek, A. Jarosz-Wilkolazka and A. Paszczyński, *FEMS Microbiol. Rev.*, **41**, 941 (2017).
- W. Wang, C. Zhang, X. Sun, S. Su, Q. Li and R. J. Linhardt, *World J. Microbiol. Biotechnol.*, **33**, 125 (2017).
- C. Alvarez-Vasco, R. Ma, M. Quintero, M. Guo, S. Geleynse, K. K. Ramasamy, M. Wolcott and X. Zhang, *Green Chem.*, **18**, 5133 (2016).
- M. Francisco, A. van den Bruinhorst and M. C. Kroon, *Green Chem.*, **14**, 2153 (2012).
- H. Tadesse and R. Luque, *Energy Environ. Sci.*, **4**, 3913 (2011).
- M. E. Vallejos, M. D. Zambon, M. C. Area and A. A. da Silva Curvelo, *Ind. Crops Prod.*, **65**, 349 (2015).
- N. Kvarnlöf and U. Germgård, *BioResources*, **10**, 3934 (2015).
- M. Naqvi, E. Dahlquist, A. S. Nizami, M. Danish, S. Naqvi, U. Farooq, A. S. Qureshi and M. Rehan, *Energy Procedia*, **142**, 977 (2017).
- Y. Jiang, X. Zeng, R. Luque, X. Tang, Y. Sun, T. Lei, S. Liu and L. Lin, *ChemSusChem*, **10**, 3982 (2017).
- Y. Jiang, N. Ding, B. Luo, Z. Li, X. Tang, X. Zeng, Y. Sun, S. Liu, T. Lei and L. Lin, *ChemCatChem*, **9**, 2544 (2017).
- Q. Yang, J. Shi, L. Lin, J. Zhuang, C. Pang, T. Xie and Y. Liu, *J. Agric. Food Chem.*, **60**, 4656 (2012).
- J. J. Bozell, L. Moens, D. Elliott, Y. Wang, G. Neuenschwander, S. Fitzpatrick, R. Bilski and J. Jarnefeld, *Resour. Conserv. Recycl.*, **28**, 227 (2000).
- H. Im, B. Kim and J. W. Lee, *Bioresour. Technol.*, **193**, 386 (2015).
- T. H. Kim, Y. K. Oh, J. W. Lee and Y. K. Chang, *Algal Res.*, **26**, 431 (2017).
- J. Yang, J. Park, J. Son, B. Kim and J. W. Lee, *Bioresour. Technol. Rep.*, **2**, 84 (2018).
- X. Li, T. Lei, Z. Wang, X. Li, M. Wen, M. Yang, G. Chen, X. He, Q. Guan and Z. Li, *Ind. Crops Prod.*, **116**, 73 (2018).
- C. Liu, Q. Feng, J. Yang and X. Qi, *Bioresour. Technol.*, **255**, 50 (2018).

22. J. Du, C. Xiong, B. Luo, Y. Sun, X. Tang, X. Zeng, T. Lei, S. Liu and L. Lin, *BioResources*, **12**, 5851 (2017).
23. C. Chang, P. Cen and X. Ma, *Bioresour. Technol.*, **98**, 1448 (2007).
24. G. T. Jeong and D. H. Park, *Appl. Biochem. Biotechnol.*, **161**, 41 (2010).
25. L. Peng, L. Lin and H. Li, *Ind. Crops Prod.*, **40**, 136 (2012).
26. H. Li, L. Peng, L. Lin, K. Chen and H. Zhang, *J. Energy Chem.*, **22**, 895 (2013).
27. C. Chang, G. Xu and X. Jiang, *Bioresour. Technol.*, **121**, 93 (2012).
28. D. W. Rackemann, J. P. Bartley, M. D. Harrison and W. O. Doherty, *RSC Adv*, **6**, 74525 (2016).
29. D. Ding, J. Xi, J. Wang, X. Liu, G. Lu and Y. Wang, *Green Chem.*, **17**, 4037 (2015).
30. S. Gámez, J. J. González-Cabriales, J. A. Ramírez, G. Garrote and M. Vázquez, *J. Food Eng.*, **74**, 78 (2006).
31. H. S. Kim and G. T. Jeong, *Korean J. Chem. Eng.*, **35**, 2232 (2018).
32. K. Zhong and Q. Wang, *Carbohydr. Polym.*, **80**, 19 (2010).
33. N. A. S. Ramli and N. A. S. Amin, *BioEnergy Res.*, **10**, 50 (2017).
34. C. Yang, H. L. Song, F. Chen and T. Zou, *J. Food Sci.*, **76**, C1267 (2011).
35. Y. Muranaka, T. Suzuki, H. Sawanishi, I. Hasegawa and K. Mae, *Ind. Eng. Chem. Res.*, **53**, 11611 (2014).
36. F. Shen, R. L. Smith Jr, L. Li, L. Yan and X. Qi, *ACS Sustainable Chem. Eng.*, **5**, 2421 (2017).

## Supporting Information

### Production of levulinic acid and ethyl levulinate from cellulosic pulp derived from the cooking of lignocellulosic biomass with active oxygen and solid alkali

Chen Gong<sup>\*</sup>, Junnan Wei<sup>\*</sup>, Xing Tang<sup>\*,\*\*,†</sup>, Xianhai Zeng<sup>\*,\*\*</sup>, Yong Sun<sup>\*,\*\*</sup>, and Lu Lin<sup>\*,\*\*,†</sup>

<sup>\*</sup>Xiamen Key Laboratory of Clean and High-valued Applications of Biomass, College of Energy, Xiamen University, Xiamen 361102, China

<sup>\*\*</sup>Fujian Engineering and Research Center of Clean and High-valued Technologies for Biomass, Xiamen 361005, Fujian, China

(Received 3 November 2018 • accepted 11 March 2019)

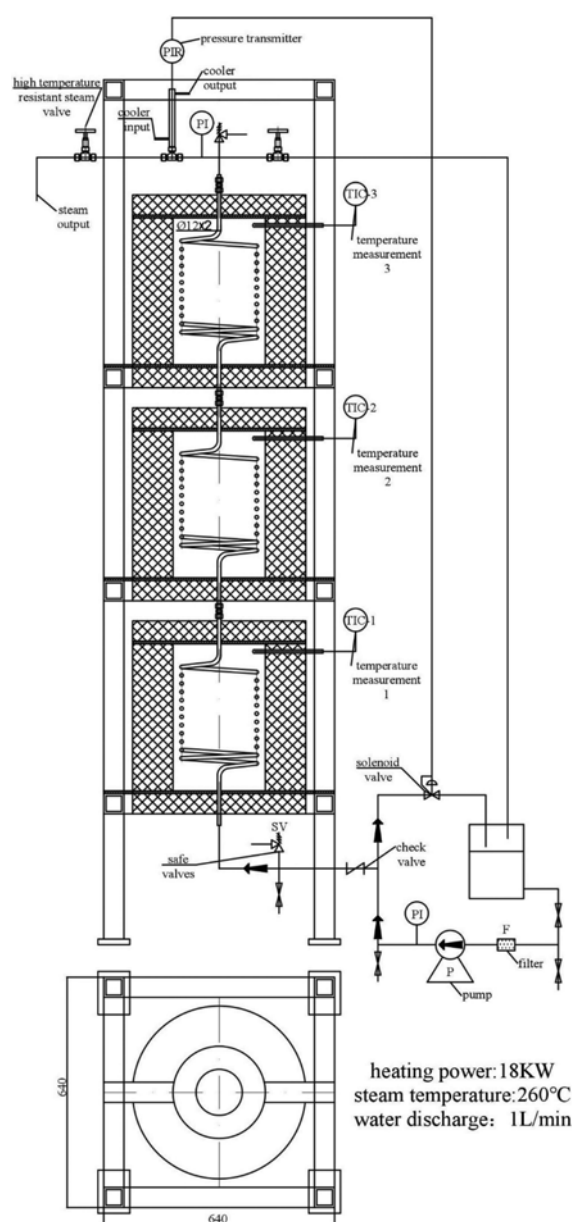
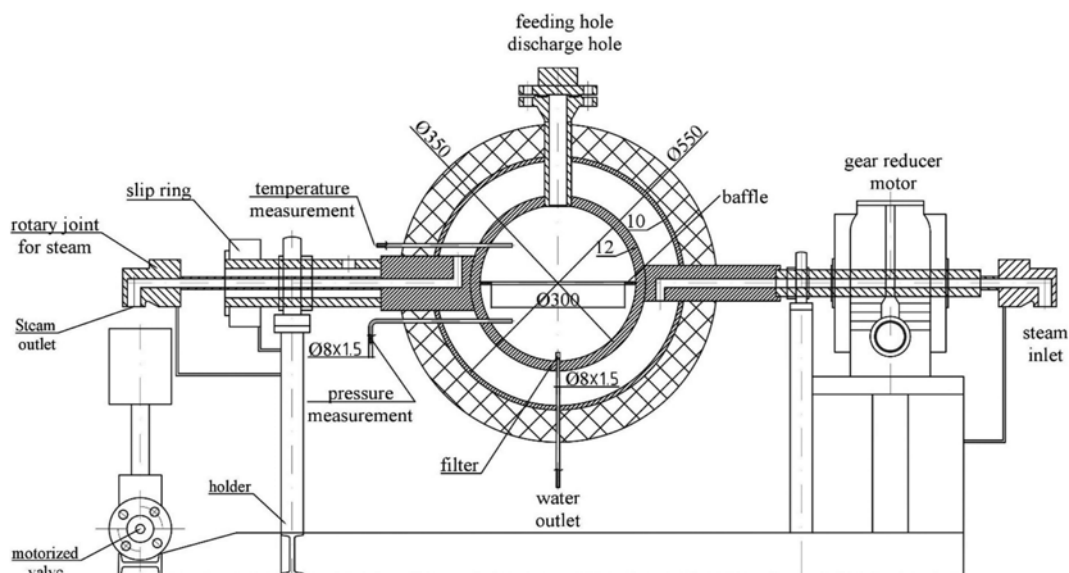


Fig. S1. Structure of the heater of ball-shaped reactor.

**Table S1. Representative literatures for the production of LA or EL from cellulose or biomass with pretreatment**

Material	Pretreatment	Solvent	Catalyst	LA/EL yield (%)	Reference
Cellulose	Acidic hydrothermal	Water	Phosphoric acid	48.2	[35]
Cellulose	Acidic hydrothermal	Water	Hydrochloric acid	59.1	[35]
Cellulose	Ionic liquid	Water	Sulfuric acid	72.9	[35]
Cellulose	Ball-milling	Water	SA-SO <sub>3</sub> H solid acid	52.2	[36]
Bamboo	CAOSA	Water	Sulfuric acid	65.3	This work
Bamboo	\	Water	Sulfuric acid	54.7	This work
Duckweed	\	Ethanol	Sulfuric acid	55.2	[21]
Wheat straw	\	Ethanol	Sulfuric acid	51.0	[27]
Bamboo	\	Ethanol	Sulfuric acid	51.3	This work
Bamboo	CAOSA	Ethanol	Sulfuric acid	62.7	This work



**Fig. S2. Structure of the kettle of ball-shaped reactor.**

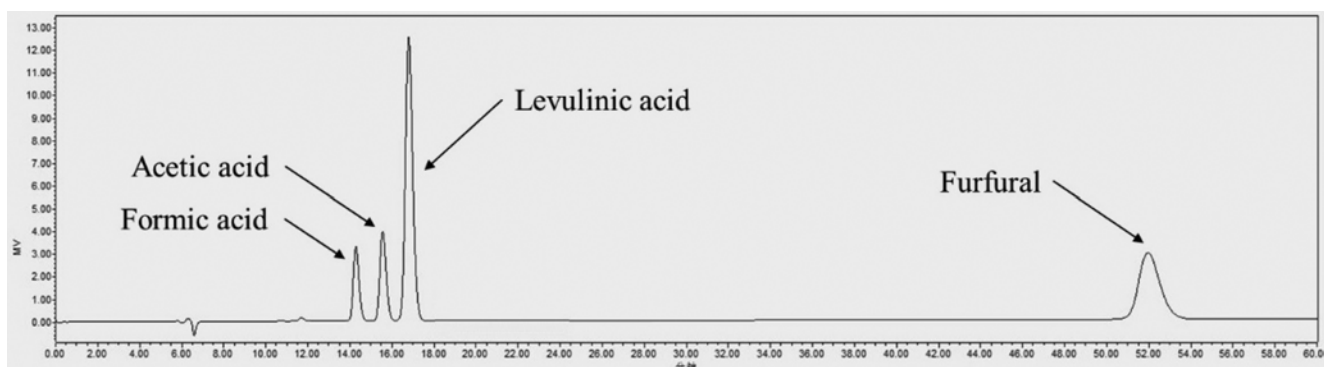


**Fig. S3. Typical liquid chromatogram of major products in biomass hydrolysate.**

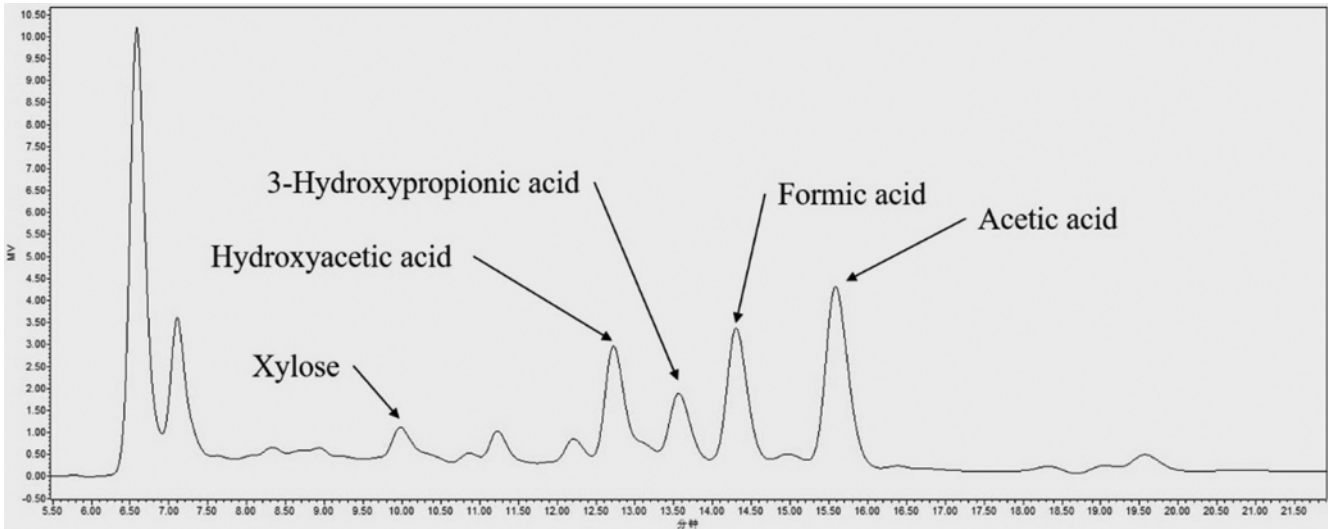


Fig. S4. Liquid chromatogram of products in water phase from CAOSA process.

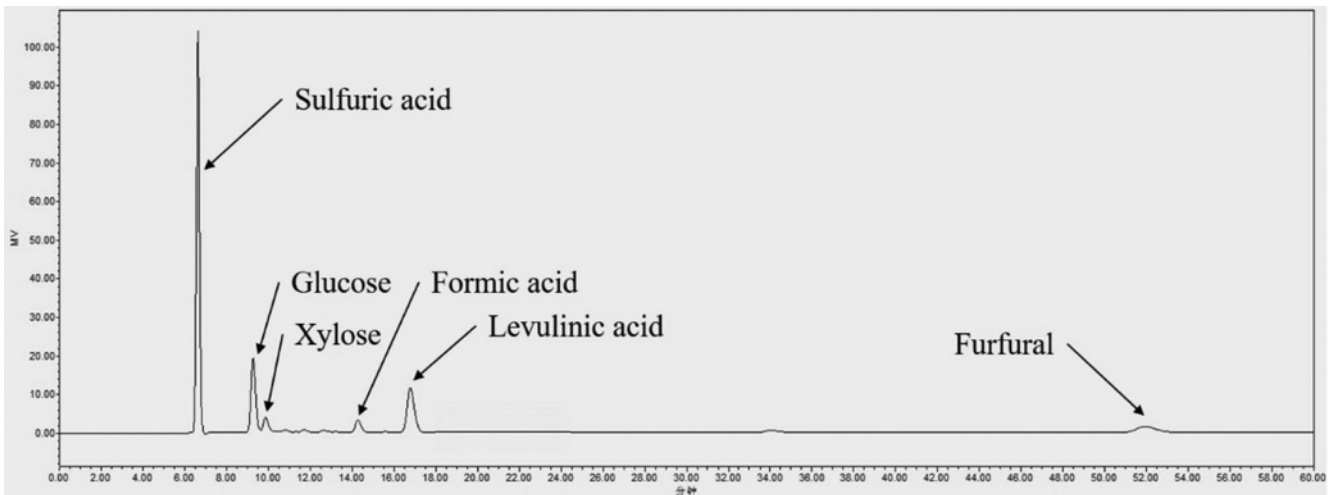


Fig. S5. Liquid chromatogram of products obtained after the reaction temperature reached 200 °C.